Oocyte-Secreted Growth Differentiation Factor 9 Inhibits BCL-2-Interacting Mediator of Cell Death-Extra Long Expression in Porcine Cumulus Cell

Author(s): Xian-Long Wang , Kun Wang , Shuan Zhao , Yi Wu , Hui Gao , and Shen-Ming Zeng
Source: Biology of Reproduction, 89(3) 2013.
Published By: Society for the Study of Reproduction
URL: http://www.bioone.org/doi/full/10.1095/biolreprod.113.108365

BIOLOGY OF REPRODUCTION (2013) **89**(3):56, 1–9
Published online before print 10 July 2013.
DOI 10.1095/biolreprod.113.108365

Oocyte-Secreted Growth Differentiation Factor 9 Inhibits BCL-2-Interacting Mediator of Cell Death-Extra Long Expression in Porcine Cumulus Cell[1]

Xian-Long Wang,[3,4,5] Kun Wang,[3,4] Shuan Zhao,[4] Yi Wu,[4] Hui Gao,[4] and Shen-Ming Zeng[2,4]

[4]*Laboratory of Animal Embryonic Biotechnology, College of Animal Science and Technology, China Agricultural University, Beijing, China*
[5]*State Key Laboratory of Reproductive Biology, Institute of Zoology, Chinese Academy of Sciences, Beijing, China*

ABSTRACT

Oocyte-secreted factors (OSFs) maintain the low incidence of cumulus cell apoptosis. In this report, we described that the presence of oocytes suppressed the expression of proapoptotic protein BCL-2-interacting mediator of cell death-extra long (BIM_{EL}) in porcine cumulus cells. Atretic (terminal deoxynucleotidyl transferase dUTP nick end labeling-positive) cumulus cells strongly expressed BIM_{EL} protein. The healthy cumulus-oocyte complex exhibited a low BIM_{EL} expression in cumulus cell while the removal of oocyte led to an about 2.5-fold ($P < 0.5$) increased expression in oocytectomized complex (OOX). Coculturing OOXs with denuded oocytes decreased BIM_{EL} expression to the normal level. The similar expression pattern could also be achieved in OOXs treated with exogenous recombinant mouse growth differentiation factor 9 (GDF9), a well-characterized OSF. This inhibitory action of GDF9 was prevented by the addition of a phosphatidylinositol 3-kinase (PI3K) inhibitor LY294002. Luciferase assay further demonstrated that *BIM* gene expression was forkhead box O3a (FOXO3a)-dependent because mutation of FOXO3a-binding site on the *BIM* promoter inhibited luciferase activities. Moreover, the activity of *BIM* promoter encompassing the FOXO3a-binding site could be regulated by GDF9. Additionally, we found that GDF9 elevated the levels of phosphorylated AKT and FOXO3a, and this process was independent of the SMAD signal pathway. Taken together, we concluded that OSFs, particularly GDF9, maintained the low level of BIM_{EL} expression in cumulus cell through activation of the PI3K/FOXO3a pathway.

apoptosis, atresia, BIM, cumulus cell, cumulus cells, GDF9, oocyte-follicle interactions, porcine/pig

INTRODUCTION

Mammalian ovarian follicle, a highly specialized structure, which consists of an oocyte surrounded by cumulus, granulosa, and thecal cells, represents the basic functional unit of the ovary. Normal folliculogenesis requires bidirectional paracrine signaling between oocytes and companion somatic cells [1–5]. Mural granulosa cell and cumulus cells provide the necessary stimulus for oocyte growth and acquisition of developmental competence [6, 7]. Recently, many studies using oocytes and granulosa cells to reconstitute follicles have demonstrated that it was oocytes that orchestrated and coordinated the development of mammalian ovarian follicles and that the rate of follicle development was controlled by the oocyte [8]. Therefore, paracrine signals derived from oocytes play dominant roles in determining the mural granulosa and cumulus cell proliferation, differentiation, and metabolism. For example, oocyte-secreted factors (OSFs) act locally to promote follicular formation and transition [9, 10], cumulus expansion [11], and several metabolic processes [12, 13] in cumulus cells. In additional, OSFs were also found to maintain the low incidence of cumulus cell apoptosis [14], which might be part of the reason that cumulus cells remain healthy within antral atretic follicles [15, 16]. However, currently there is little data available as to whether OSFs can suppress apoptosis-related gene expression in cumulus cells.

The mechanisms by which mural granulosa and cumulus cells survive and escape from apoptosis are not fully defined but involve BCL-2 family proteins [17], which are gatekeepers of the apoptotic machinery and possess up to four conserved BCL-2 homology (BH) domains [18]. Family members such as BCL-2 are antiapoptotic, whereas others such as BCL-2-interacting mediator of cell death (BIM), with a single BH3 domain, are proapoptotic [19]. In adult female mouse, moderate BIM protein and *BIM* mRNA expression were observed within the granulosa cells of primordial, primary, secondary, and mature follicles [20]. Our previous studies have demonstrated that BIM-extra long (BIM_{EL}), the predominant isoform of BIM, could induce apoptosis in porcine mural granulosa cell and was reduced by follicle-stimulating hormone (FSH) [21]. Furthermore, Wu et al. [22] reported that BIM_{EL} protein expression and apoptosis in porcine cumulus cells progressively increased along with cumulus-oocyte complexes (COCs) cultured time. However, a precise study of this phenomenon has yet to be described.

FSH and oocyte factors are the critical regulators of follicular cell function [23] and signal from opposite compartments. The FSH signals display a centripetal pattern from outside of a follicle, whereas oocyte signals emanate from a central follicular location [24]. FSH signals through phosphatidylinositol 3-kinase (PI3K), and oocyte factors signal through Sma- and Mad-related (SMAD) protein. This suggests that the follicular development requires cross-talk between PI3K and SMAD signals. It recently has been demonstrated that, apart from the classical SMAD signal transduction pathway, OSF, growth differentiation factor 9 (GDF9), has been shown to also activate a large number of parallel noncanonical signaling pathways, including ERK1/2 [25], p38 MAPK [26], and PI3K [27], all of which are involved in regulating BIM_{EL} protein expression [28]. Consequently, we speculate that the oocytes can protect cumulus cells from

[1]Supported by a National Natural Science Foundation of China Grant 31072031.
[2]Correspondence: Shen-Ming Zeng, Dongke Building #251, NO. 2 Yuanmingyuan West Road, Haidian District, Beijing 100193, China. E-mail: zengsm@cau.edu.cn.
[3]These authors contributed equally to this work.

Received: 31 January 2013.
First decision: 8 March 2013.
Accepted: 24 June 2013.

eISSN: 1529-7268 http://www.biolreprod.org
ISSN: 0006-3363

undergoing apoptosis by suppressing BIM_{EL} protein expression. To test this hypothesis, we first analyzed BIM_{EL} protein level in cumulus cells cultured alone or with denuded oocytes (DOs). Then, the possible involvement of GDF9 in BIM_{EL} expression was investigated on cumulus cells cultured with recombinant mouse GDF9. Lastly, we pursued the signaling pathway involved in this process.

MATERIALS AND METHODS

Unless otherwise specified, all the chemicals used in this study were purchased from Sigma-Aldrich.

Collection of Porcine Cumulus-Oocyte Complexes

Porcine ovaries were collected at a local abbatoir and transported to the laboratory in a thermos flask at 35°C–37°C in sterile physiological saline within 4–6 h after the animals were slaughtered. At the laboratory, ovaries were washed twice with 37°C sterile physiological saline (containing 100 international units/L penicillin and 50 mg/L streptomycin). COCs were aspirated from follicles (2–6 mm in diameter) with an 18-gauge needle attached to a disposable 10 ml syringe. After being washed three times with Tyrode lactate-Hepes-0.1% polyvinyl alcohol, the COCs were collected as healthy (H) and atretic (A) groups according to the method of Boni et al. [29] as follows: H-COC, presence of a clear and compact cumulus and a translucent ooplasm; and A-COC, dark and anomalous cumulus and dark ooplasm (Fig. 1A). Only H-COCs were used to generate oocytectomized complexes (OOX) and DOs.

Coculture of Oocytectomized Complexes with DOs

The cytoplasm of each oocyte was microsurgically removed from the COC (oocytectomy) using a micromanipulator. The resulting OOX consists of a hollow zona pellucida surrounded by several layers of intact cumulus cells. The DOs were generated by gentle pipetting in 0.1% hyaluronidase and washed three times in M199 (Earle salt with 25 mM Hepes buffer) supplemented with 0.5% fetal bovine serum (FBS). The oocytes with no remaining cumulus cells were selected and used.

COCs (n = 10), OOXs (n = 10), and OOXs plus DOs (n = 10 and 50, respectively) were cultured in a droplet (10 μl) of medium covered with mineral oil in a 35 mm dish (Nuclon). In some experiments, the numbers of DOs in coculture system were indicated. The culture medium was MEM ALPHA (Invitrogen Corporation) supplemented with 100 units/ml penicillin and 50 mg/ml streptomycin.

Treatment with Inhibitors

In the case of treatment with each specific inhibitor, OOXs were pretreated with each of these inhibitors for 1 h before the addition of GDF9 or DOs. The working concentration of each inhibitor used in the present study was commonly used and well confirmed in mammalian ovarian cell studies [30–32]. H89 (PKA inhibitor) was dissolved in culture medium at 20 mM and stored at −20°C. SB203580 (p38MAPK inhibitor, 20 mM), LY294002 (PI3K inhibitor, 20 mM), PDTC (NF-κB inhibitor, 200 mM), and SB431542 (SMAD inhibitor, 10 mM) were dissolved in dimethylsulfoxide (DMSO) and stored at −20°C. The working concentrations of these inhibitors were obtained by dilution (1:1000) with the culture medium.

RNA Isolation and Reverse Transcription-PCR

Following culture treatments, total cellular RNA from OOX complexes was extracted using an RNAprep pure tissue kit (TIANGEN Biotech) according to the manufacturer's instructions. Total RNA content was determined by spectrophotometry (260 nm) and used for cDNA synthesis (RevertAid First Strand cDNA Synthesis Kit; Thermo Fisher Scientific). Amplification reactions were performed in 25 μl reaction volume containing 1 μl cDNA, 12.5 μl of 2 × PCR master mix (TIANGEN Biotech), 10.5 μl sterile water, and 0.5 μl each of forward and reverse *BIM* gene-specific primers (10 μM): forward 5′-TGAGGCAGTCTCAGGCTGAACCC-3′ and reverse 5′-ATACGCCGTAACTCCTGCGCAAT-3′. Thermal cycling conditions were 94°C for 2 min; followed by 30 cycles at 94°C for 30 sec, 59°C for 30 sec, and 72°C for 30 sec; and finally, 72°C for 10 min. The products were separated by electrophoresis on a 1.5% agarose gel. Reactions were performed in triplicate.

Western Blot Analysis

Following culture treatments, OOX complexes were lysed in Laemmli sample buffer (Bio-Rad). In some experiments, the cytoplasm of oocyte was microsurgically removed from the COCs before OOX complexes were lysed. Proteins from an equal number of OOXs were separated by SDS-PAGE (12% acrylamide running gel) and transferred to a nitrocellulose membrane (BioTraceNT; Pall). Nonspecific binding to the membrane was blocked with 5% nonfat milk in 10 mM Tris, pH 7.5, 150 mM NaCl, and 0.1% Tween 20 at room temperature for 1h. Membranes were then incubated with primary antibodies (4°C, overnight), followed by incubation with horseradish peroxidase-conjugated secondary antibodies for 1h at room temperature. Antibodies against BIM (1:2000 dilution, product no. 2933) and Phospho-FOXO3a (1:1000 dilution, product no. 9466) were purchased from Cell Signaling Technology. Antibodies against ACTIN (1:500 dilution, product no. sc-47778), AKT (1:500 dilution, product no. sc-8312), and Phospho-AKT (1:500 dilution, product no. sc-16646-R) were purchased from Santa Cruz Biotechnology. Horseradish peroxidase-conjugated secondary antibody (rabbit: 1:5000 dilution, product no. ZB-2301; mouse: 1:5000 dilution, product no. ZB-5305) were purchased from ZSGB-Bio. The protein bands were visualized by enhanced chemiluminescence detection reagents (Applygen Technologies Inc.) and X-Omat BT film (Eastman Kodak Co.), according to the manufacturers' instructions. The films were digitized, and densitometry analysis was performed with ImageJ 1.44p software (National Institutes of Health). The relative intensity of the bands was quantified and normalized to the respective loading control. In BIM_{EL} immunoblots system, a prominent shift in the electrophoretic mobility was attributed to a different degree of phosphorylation [21], and the sum of relative intensity of all the bands were quantified.

Histology (Immunofluorescence and Terminal Deoxynucleotidyl Transferase dUTP Nick End Labeling)

Cumulus cell apoptotic DNA was detected using in situ Cell Death Detection Kit (Roche Diagnostic) according to the manufacturer's instructions. Following culture treatments, OOX complexes were washed twice in PBS (pH 7.4) containing 1% bovine serum albumin (BSA), fixed in 4% paraformaldehyde in PBS (pH 7.4) at 4°C overnight. Complexes were then permeabilized in 0.5% Triton X-100 solution at 4°C for 1 h and washed three times in PBS/BSA. The complexes were then incubated in fluorescein-conjugated dUTP and terminal deoxynucleotide transferase (terminal deoxynucleotidyl transferase dUTP nick end labeling [TUNEL] reagents; Roche) at 37°C in the dark for 1 h. After incubation with 10 μg/ml Hoechst 33342 for 10 min, complexes were washed and mounted on glass slides and observed under a Leica fluorescence microscopy. A percentage of apoptotic nuclei (TUNEL-positive) were counted at a magnification of ×100, and the three percentile values were then averaged to achieve a representation of the total apoptotic nuclei percentage.

Small Interfering RNAs and Transfection

Control small interfering RNA (siRNA) (mock), 5′-UUCUCCGAACGUGUCACGUTT-3′, and one validated siRNA against porcine *AKT* (si*AKT*, 5′-GGCCCAACACCUUCAUCAUTT-3′) were designed and synthesized by GenePharma. The cumulus cell monolayers were established as described [33]. Briefly, oocytes were denuded by pipetting, and the cells were placed in Dulbecco modified Eagle culture medium plus 10% FBS (Hyclone) and supplemented with 100 units/ml penicillin and 50 mg/ml streptomycin at 37.5°C in a humidified atmosphere of 5% CO_2. After 4 days in culture, cumulus cell monolayers formed and were cultured to confluence. To passage the cells, confluent cells were disaggregated by incubation in 0.1% trypsin and 0.02% ethylenediaminetetraacetic acid solution at 37°C for 1 min and then seeded in 35 mm dishes and grown to 30%–50% confluence. Cells were then incubated in antibiotic-free medium overnight, followed by transfection with 10 pmol of siRNA duplex using Lipofectamine RNAiMAX (Invitrogen) according to the manufacturer's instructions. Total protein was prepared at 48 h after transfection and was used for Western blot analysis.

Plasmid Preparation and Dual-Luciferase Reporter Assays

As described previously [21], a 1213-bp nucleotide (nt) fragment containing the region between −1151 and +62 of the *BIM* gene upstream from the translational start codon was cloned from porcine genomic DNA by PCR amplification. The oligonucleotide primers listed in Supplemental Table S1 were used to generate a series of *BIM* promoter pGL3 luciferase reporter vectors (all the supplemental data is available at www.biolreprod.org). The PCR products were digested with *Sac*I and *Hind*III restriction enzymes and cloned into the *Sac*I and *Hind*III sites of the pGL3-Basic vector (Promega). The

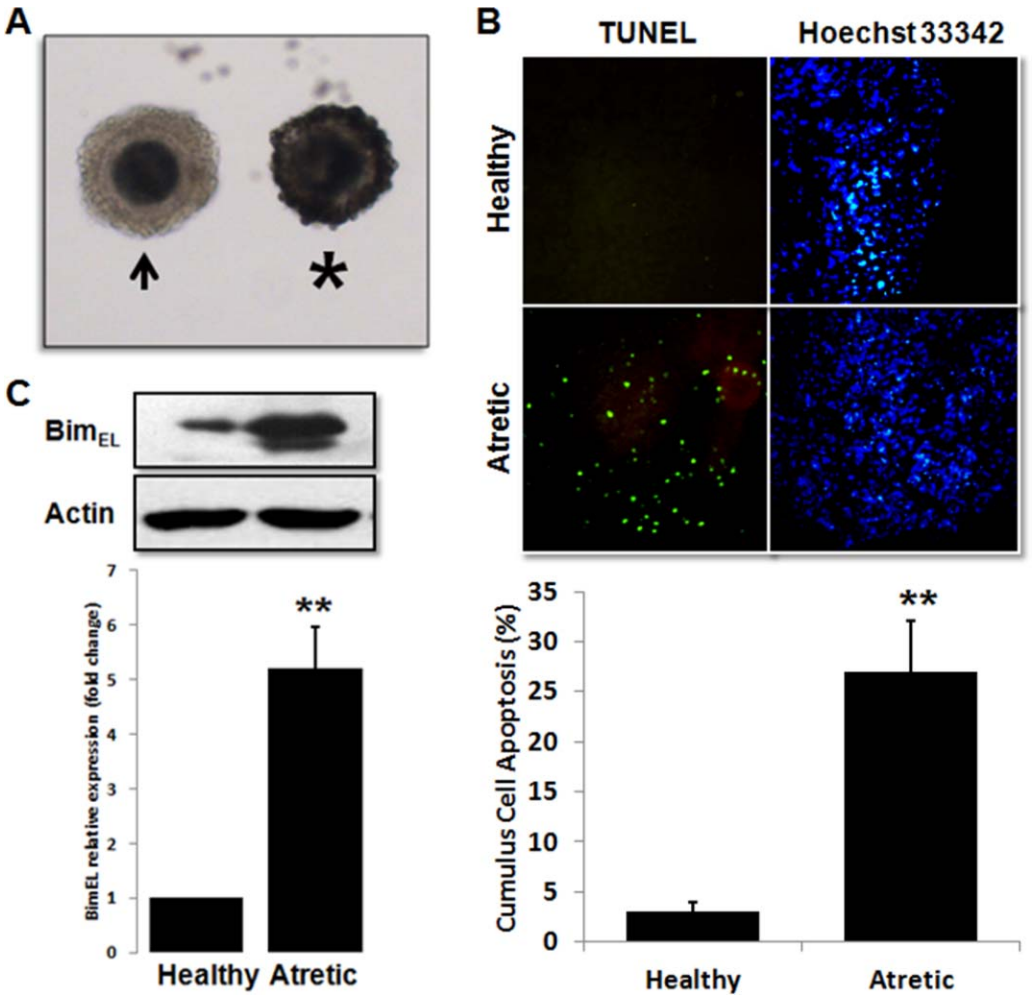

FIG. 1. Porcine cumulus cell apoptosis is related to increasing BIM_{EL} expression. **A**) Representative image showing healthy (*arrow*) and atretic (*asterisk*) cumulus-oocyte complex (COC). **B**) The incidence of cumulus cell apoptosis in H- and A-COCs. *Top panel,* fluorescence microscopy of DNA fragmentation in cumulus cells as detected by TUNEL (green label). All the cell nuclei were also stained with Hoechst 33342 (blue). *Bottom panel,* quantitative comparison of cumulus cell apoptosis between H- and A-COCs. Values represent means ± SEM of three independent experiments. $^{**}P < 0.01$. **C**) Isolated cumulus cell lysates, obtained from H- or A-COCs were subjected to immunoblotting to detect BIM_{EL} expression. Actin was used as fractionation control. A representative blot is shown. The graph demonstrates the results of the densitometric analysis of BIM_{EL} protein levels normalized against loading controls (arbitrary units, healthy = 1). Values represent means ± SEM of three experiments. $^{**}P < 0.01$.

plasmid was propagated using DH5α (TIANGEN Biotech) as the host strain and purified with an EndoFree Plasmid maxi kit (Qiagen Inc.). Mutation in the FOXO3a-binding site was generated using a QuikChange XL Site-Directed Mutagenesis kit (Stratagene) according to the manufacturer's instructions. The oligonucleotides 5′-AGTCACTCCAGTCCCAACGCCCGGCGGGG-3′ and 5′-CCCCGCCGGGCGTTGGGACTGGAGTGACT-3′ were used. Sequencing confirmed that all the constructs had been incorporated correctly.

For the dual-luciferase reporter assays, cumulus cells were transfected with 1 μg of a luciferase reporter plasmid and 100 ng of the pRL-CMV *Renilla* luciferase reporter plasmid (Promega). After 24 h transfection, cell lysates were prepared from each sample, and luciferase activity was detected using the Dual-Luciferase reporter assay system (Promega) and a Turner Design TD-20/20 luminometer (Jencons Scientific Limited). *Firefly* output was normalized to *Renilla* output to control for transfection efficiency.

In Silico Analysis

Putative transcription factor binding sites were searched by Consite (http://asp.ii.uib.no:8090/cgi-bin/CONSITE/consite) using the default settings.

Statistical Analyses

Data of the apoptosis, amounts of protein expression and luciferase activity were analyzed using a general linear model and one-way post hoc test using the MIXED procedure models of SAS (version 9.1; SAS Institute Inc.). The results are represented as means ± SEM. Statistical significance was determined by a value of $P < 0.05$ for all the analyses.

RESULTS

Increased BIM_{EL} Expression Is Associated with Cumulus Cell Apoptosis

The incidence of apoptosis in cumulus cells from H-COCs and A-COCs were investigated. As shown in Fig. 1B, the incidence of cumulus cell apoptosis, demonstrated by TUNEL assay in A-COCs was significantly higher compared with that of H-COCs ($P < 0.01$). In accordance with the results obtained by TUNEL, a higher BIM_{EL} protein expression in cumulus cells was observed in A-COCs compared with that of H-COCs (Fig. 1C).

The Effect of Oocyte Factors on BIM_{EL} Expression in Cumulus Cell

To investigate whether the presence of oocyte is responsible for low BIM_{EL} expression in cumulus cell from H-COCs, DOs

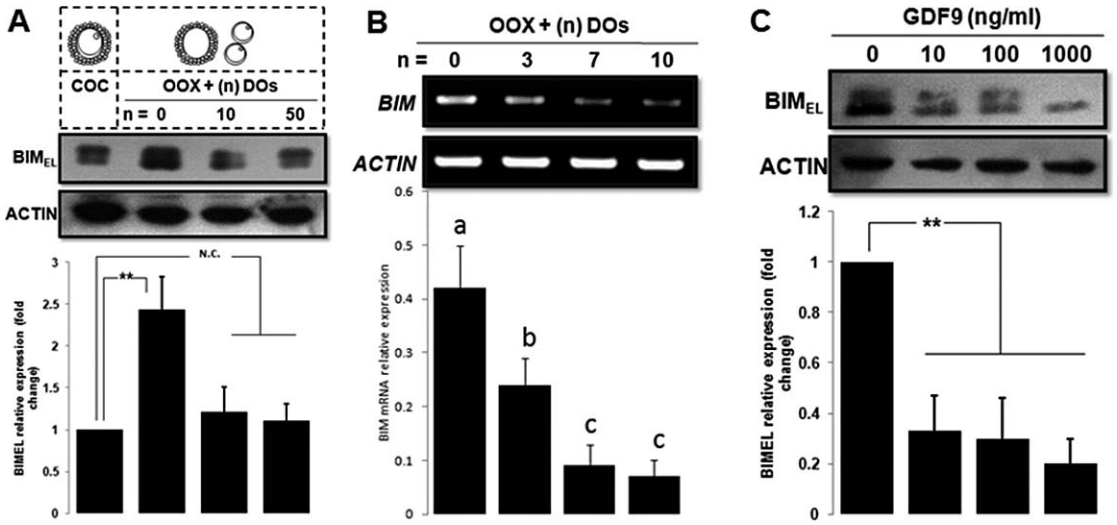

FIG. 2. The effect of oocyte factors on BIM_{EL} expression in cumulus cell. Ten oocytectomized complexes (OOX) were cultured under basal conditions (10 μl medium per microdrop) with the indicated the number of denuded oocytes (DOs) (**A** and **B**) or 0, 10, 100, and 1000 ng/ml GDF9 (**C**) for 18 h. BIM_{EL} protein and transcripts levels in cumulus cells were assessed by immunoblotting and RT-PCR, respectively. Actin was used as fractionation control. Representative pictures are shown. The graph demonstrates the results of the densitometric analysis of BIM_{EL} expression levels. COC and GDF9: 0 ng/ml = 1 (arbitrary units) in **A** and **C**. Values represent means ± SEM of three experiments. $^{**}P < 0.01$. $^{a–c}$Means without a common superscript differ ($P < 0.05$).

were isolated from H-COCs for coculturing OOXs. When cultured under basal conditions, BIM_{EL} expression in OOX cumulus cells was increased compared with cumulus cells cultured as intact COCs (Fig. 2A). Coculturing OOX cumulus cells with DOs (10 or 50 per microdrop) reduced BIM_{EL} expression to the same normal low level as intact H-COCs (Fig. 2A). Furthermore, we showed that oocytes could inhibit *BIM* transcripts expression in a dose-dependent manner (Fig. 2B).

To determine if oocyte paracrine factors are responsible for low BIM_{EL} expression, the OOX was cultured alone in basal conditions supplemented with GDF9, an abundant and critical OSF. Immunoblot analysis showed coincubation with GDF9 also could down-regulate BIM_{EL} expression (Fig. 2C).

PI3K Is Involved in the Inhibitory Action of Oocyte Factors on BIM_{EL} Expression

To test whether a SMAD-dependent pathway participates in the process of GDF9 suppression of BIM_{EL} expression in cumulus cells, we first examined the effect of specific inhibitors for phosphorylation of SMAD on BIM_{EL} expression of OOXs in the presence of GDF9. As shown in Figure 3A, treatment with SMAD inhibitor SB431542 (10 μM) induced 2-fold ($P < 0.05$) increase in BIM_{EL} protein expression, which was only about 45% of that seen after GDF9 withdrawal. This raises the possibility that the SMAD pathway plays a necessary, but not sufficient, role in inducing BIM_{EL} expression.

To gain insight into the underlying mechanisms by which an oocyte factor (GDF9) suppress the BIM_{EL} expression in cumulus cells, intracellular signaling pathways were monitored using the specific inhibitors SB203580 (p38MAPK inhibitor), H89 (PKA inhibitor), LY294002 (PI3K inhibitor), and PDTC (NF-κB inhibitor). It was apparent that GDF9 inhibitory action on BIM_{EL} expression was abolished by pretreatment with the PI3K and NF-κB inhibitors (Fig. 3B). In the present study, we just focused on the PI3K pathway because it was involved in the survival and metabolism of cumulus cells [34, 35].

To further specify the PI3K involved in the inhibitory action of oocyte factors on BIM_{EL} expression, the OOXs plus DOs or intact COCs were cultured under basal conditions in the presence of vehicle (DMSO) or LY294002 (20 μM). In immunoblotting experiments, incubation with LY294002 caused a significantly higher amount of BIM_{EL} protein expression in cumulus cells from OOXs (about 2.5-fold) or COCs (about 3-fold) compared with control and vehicle ($P < 0.05$) (Fig. 3C). Similarly, using immunofluorescent assay, we found that the OOXs cultured under basal conditions exhibited an intense BIM_{EL} immunostaining. Coculturing OOXs with DOs caused barely visible BIM_{EL} immunostaining. Incubation with LY294002 (20 μM) in latter system restored the intense BIM_{EL} immunostaining (Fig. 3D). Additionally, the cumulus cell apoptosis as detected by TUNEL was also associated with the same treatment (Fig. 3D). These results suggested that the inhibitory action of oocytes on BIM_{EL} expression could be dampened by LY294002.

FOXO3a-Binding Element Is Required for Activation of the BIM Promoter

To further investigate the mechanisms involved in the regulation of the *BIM* gene in cumulus cell, an 1213-bp fragment of the *BIM* promoter from nt −1151 to +62 was cloned from porcine genomic DNA and inserted into a pGL3 luciferase reporter vector. A series of *BIM* promoter luciferase reporter vectors were constructed by deleting the sequences from the 5′-flanking region of the promoter (Fig. 4A). These constructs were then transfected into cumulus cells and assayed for reporter gene activity. Truncation of the sequence between nt −433 and −254 caused about a 10-fold increase in luciferase activity (Fig. 4B), which implies the presence of a strong depressor in the region between −433 and −254. We identified a 42-bp depressor element by another series of −433 and −254 *BIM* promoter luciferase reporter vectors (Supplemental Fig. S1). Sequence alignment revealed that 15 bases of this element were conservative compared to its human and mouse counterparts (Supplemental Fig. S2).

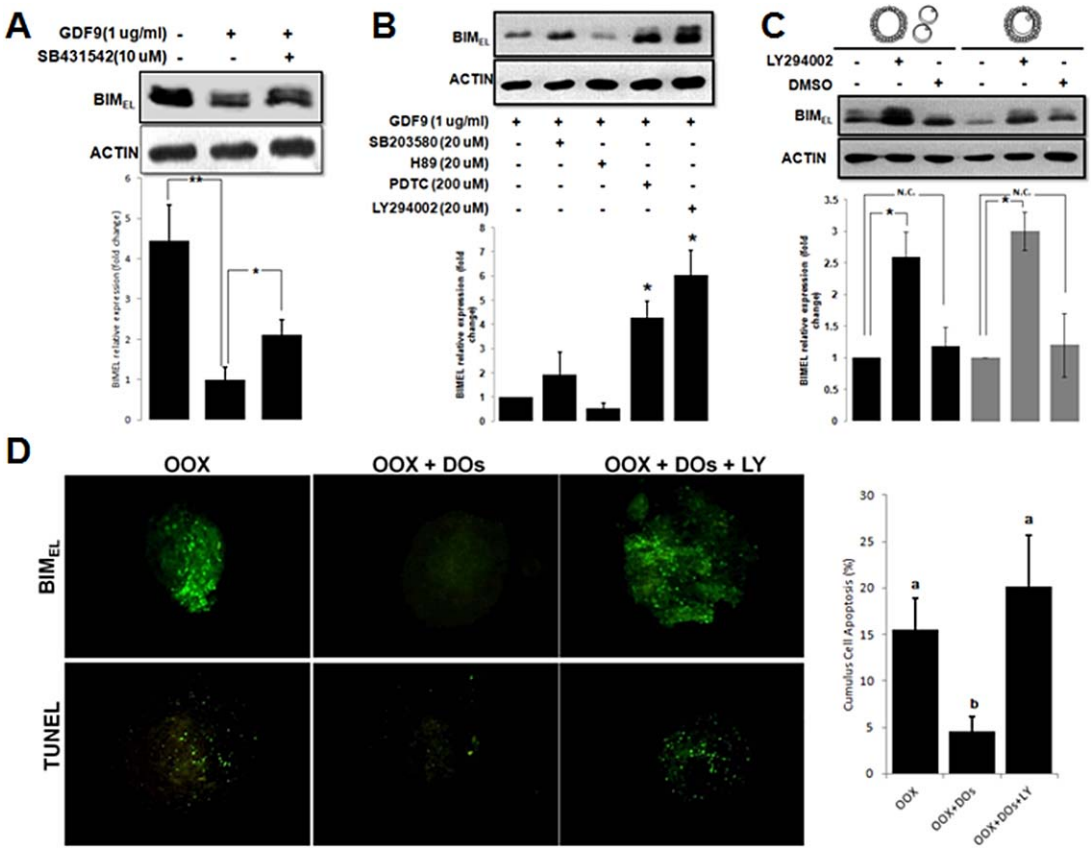

FIG. 3. Phosphatidylinositol 3-kinase (PI3K) is involved in the inhibitory action of oocyte factors on BIM_{EL} expression. **A**) Oocytectomized complexes (OOX) were cultured under basal conditions. SMAD-specific inhibitor SB431542 (10 μM) was added 1 h before the incubation with DOs. **B**) Selective specific inhibitors of p38MAPK (SB203580; 20 μM), PKA (H89; 20 μM), NF-κB (PDTC; 200 μM), and PI3K (LY294002; 20 μM) were added 1 h before treatment with GDF9 (1 μg/ml). **C**) OOXs plus DOs or COCs were treated with LY294002 (20 μM) or DMSO (vehicle). For OOXs plus DOs, LY294002 or DMSO was added 1 h before the addition of DOs. The indicated protein levels in cumulus cells were assessed by immunoblotting after 18 h incubation. Actin was used as the fractionation control. A representative blot is shown. The graph demonstrates the results of the densitometric analysis of protein levels normalized against loading controls (arbitrary units, nontreatment, GDF9 only, OOXs plus DOs only and COCs only = 1, respectively). Values represent means ± SEM of three experiments. $^*P < 0.05$. **D**) Fluorescence microscopy of BIM_{EL} immunofluorescence and DNA fragmentation (detected by TUNEL) in cumulus cells with the same treatment as above. The graph demonstrates the quantitative estimation of cumulus cell apoptosis. Bars with different superscripts are significantly different at $P < 0.05$.

A significant reduction in luciferase activity was observed when the 5′-flanking region was shortened from position −254 to −115 (Fig. 4B). The in silico analysis of the −254 and −115 bp region of *BIM* promoter revealed a consensus FOXO3a-binding element (5′-GTAAACA-3′) [36] located at approximately −178 to −172 position. To determine whether the element is responsible for activation of the *BIM* promoter, we used site-directed mutagenesis to specifically mutate this element (Fig. 4C). As expected, mutation of the FOXO3a-binding element resulted in a significantly attenuation of *BIM* promoter activity (Fig. 4C). In addition, we also found that −254 and +62 bp region-dependent activation could be reduced by exogenous GDF9 treatment (Fig. 4D).

GDF9 Induces Phosphorylation of AKT and FOXO3a Independent of SMAD Pathway

To determine whether GDF9 activates PI3K pathways, OOXs were incubated with GDF9 (1 μg/ml) for various durations (0, 0.5, 2, and 4 h), and phospho-AKT (p-AKT) and phospho-FOXO3a (p-FOXO3a) contents were examined by Western blot analysis. Low levels of p-AKT and p-FOXO3a were detected in the absence of GDF9. As shown in Figure 5A, GDF9 increased p-AKT and p-FOXO3a contents in cumulus cells in a time-dependent manner. To further confirm the involvement of PI3K pathway in regulating BIM_{EL} expression, siRNA targeting the *AKT* gene, a downstream substrate of PI3K, was used to transfect cumulus cells. *AKT* gene knockdown using siRNA also significantly increased BIM_{EL} expression (Supplemental Fig. S3).

To determine whether the SMAD signal pathway is required for PI3K pathway activation, we determined the effect of SB431542 on the FOXO3a phosphorylation in the presence of GDF9. As shown in Figure 5B, treatment with SMAD inhibitor SB431542 (10 μM) failed to abolish phosphorylation of FOXO3a induced by GDF9.

DISCUSSION

Oocytes play a critical role in follicular cell function, such as granulosa cell proliferation, preantral follicle growth, and cumulus cell expansion. Orisaka et al. [27] showed that GDF9 promoted follicular survival and growth during the preantral to early antral transition by suppressing granulosa cell apoptosis. In the present study, we have demonstrated that the OSF inhibited porcine cumulus cell apoptosis by suppressing proapoptotic protein BIM_{EL} expression.

As a proapoptotic protein, BIM_{EL} was highly expressed in

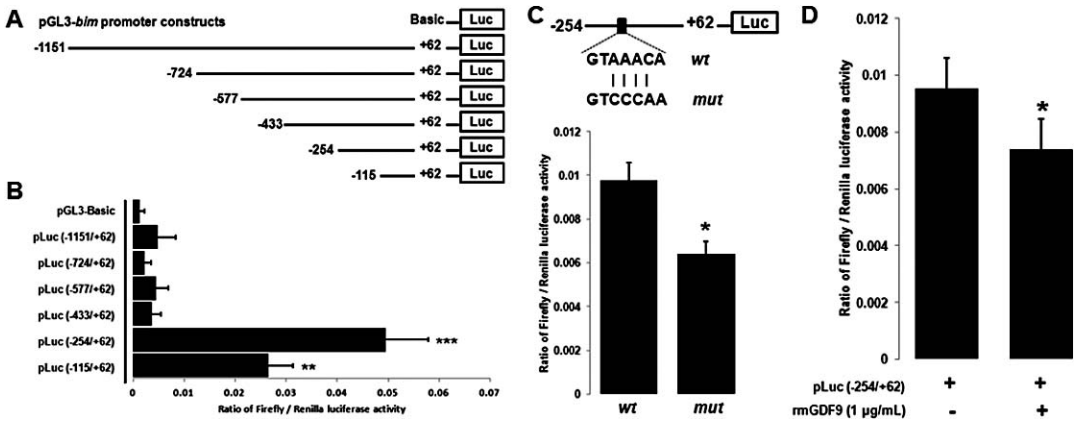

FIG. 4. FOXO3a-binding site is required for activation of the *BIM* promoter. **A**) Schematic of *BIM* promoter luciferase reporter vector constructs deleted from the 5′ region of the promoter. **B**) Relative activities of *BIM* promoter-driven luciferase gene expression in constructs from serial deletions of the promoter. **C**) FOXO3a-binding site mutation reduces *BIM* promoter (−254/+62) activity. Mutation of FOXO3a-binding site was indicated in upper panel. **D**) The effect of GDF9 on the *BIM* promoter (−254/+62) activity. Cumulus cells were cotransfected with the *Firefly* luciferase reporter and a *Renilla* luciferase internal control (pRL-CMV). The promoter activity was obtained by normalizing the *Firefly* luciferase activity to the *Renilla* luciferase activity. Values represent means ± SEM of three experiments. $^{*}P < 0.05$. $^{**}P < 0.01$. $^{***}P < 0.001$.

atretic cumulus cells that exhibited more apoptotic cells (TUNEL-positive) in our present results. Nevertheless, according to previous research [15, 16], no apoptotic cumulus cells in COCs from atretic follicles were observed. The reason may be the different criteria to classify follicles or COCs as healthy or atretic. In their studies, follicles that had no vascularized (pink or red) theca interna and clear amber follicular fluid were classified as atretic. However, in these atretic follicles that fit the above characteristics, the intact COCs are still preserved [16, 37]. Even in the severely atretic follicles, no apoptotic cumulus cells were observed in COCs that were already suspended in follicular fluid [37]. These results suggested that the cumulus cell apoptosis was inhibited by the oocyte at the early stage of atresia. Once apoptosis was initiated in the COC, the entire process of follicular atresia was terminated [16]. In present studies, we classified the COCs grade according to the COCs instead of the follicular surface morphology. We found the COCs with dark and anomalous cumulus and dark ooplasm exhibited strong TUNEL staining and high BIM_{EL} expression level.

The present study demonstrated that removal of the oocyte from the COC led to an increased BIM_{EL} expression. However, the BIM_{EL} expression level could be decreased by coculturing OOX with oocytes. These findings demonstrated that the low level of BIM_{EL} expression was largely dependent on the presence of the oocyte. Hussein et al. [14] had concluded that the effect in this culture system could be specifically attributed to soluble paracrine signals from the oocyte, rather than oocyte gap junctional signaling to cumulus cells. Recently, members of the transforming growth factor β (TGFβ) superfamily, such as GDF9 [38] and bone morphogenetic protein 15 (BMP15) [39], were considered as the best candidate molecules that could mimic many of the actions of oocytes on granulosa/cumulus cells in vitro. It was interesting to note that exogenous GDF9 markedly suppressed BIM_{EL} expression, suggesting that the inhibitory action was at least owed to GDF9. However, whether other TGFβ superfamily members, such as BMP15, participated in the regulation of BIM_{EL} expression remains to be resolved.

In present studies, the recombinant mouse GDF9 was employed to investigate the mechanism by which oocytes

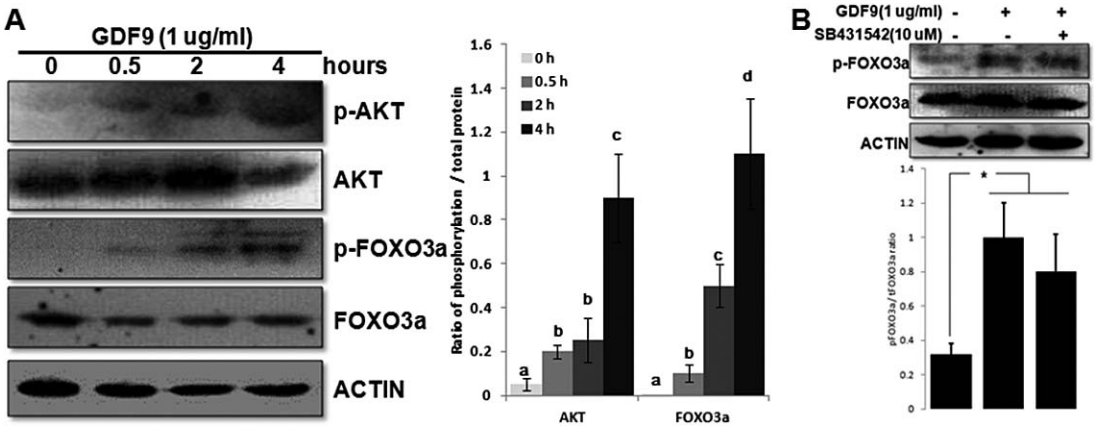

FIG. 5. GDF9 induces phosphorylation of AKT and FOXO3a independent of SMAD pathway. **A**) Oocytectomized complexes (OOX) were cultured under basal conditions for 0, 0.5, 2, or 4 h with 1 μg/ml GDF9. **B**) Oocytectomized complexes (OOX) were cultured under basal conditions. The SMAD-specific inhibitor SB431542 (10 μM) was added 1 h before the incubation with DOs. Immunoblotting analysis was completed to determine phosphorylation status of AKT and FOXO3a. The graph demonstrates the results of the densitometric analysis of protein levels. Values represented means ± SEM of three experiments. Bars with different superscripts are significantly different at $P < 0.05$.

inhibited the BIM_{EL} expression in cumulus cell in vitro. Mouse GDF9 is synthesized as a 441 amino acid (aa) prepropeptide that contains a 29 aa signal sequence, a 277 aa propeptide, and a 135 aa mature chain [40]. Amino acid residues 340–441 constitute a TGFβ-like domain, which has 93.1% homologies with its porcine counterpart [41]. Moreover, the recombinant mouse GDF9 generated in-house was reported to mimic the nonluteinizing effects of oocytes in a culture system for porcine species, especially in terms of dose-dependent increases in IGF1-stimulated granulosa cell proliferation [42].

An interesting finding in the current study was that truncation of the sequence between nt −254 and −115, which contained the FOXO3a-binding element, failed to restored the same luciferase activity level as the control. This implied the presence of some other activators in the region between −115 and +62. Recently, other transcription factors have been described to participate in the regulation of *BIM* gene transcription. Hershko and Ginsberg [43] reported that the mouse *BIM* gene promoter contained an E2F-responsive element and E2F1 overexpression up-regulated the BIM expression through a direct transcriptional mechanism in NIH3T3 cells. Hughes et al. [44] also indicated that a conserved inverted CCAAT box (ICB) in the rat *BIM* promoter was bound by the heterotrimeric transcription factor NF-Y, which cooperated with FOXO3a to recruit CBP/p300 to the *BIM* promoter to form a stable multiprotein/DNA complex that activated *BIM* transcription. In silico analysis also revealed that the potential E2F1-binding site and ICB were located at the −115 and +62 bp region of porcine *BIM* promoter, but this needs to be validated. This raises the possibility that each of the transcription factors plays a necessary, but not sufficient, role in inducing *BIM* gene expression. This is supported by the observation that the phosphorylation of FOXO3a was not affected by a SMAD inhibitor that nevertheless induces a modest increase in BIM_{EL} expression (Figs. 3A and 5B). Similar results were also obtained in sympathetic neurons, that is, BIM expression induced by inhibition of PI3K/AKT pathway is only about 60% of that seen after NGF withdrawal [45].

It is well known that the OSFs are mimicked by TGFβ superfamily members, which signal through a complex of type I (activinlike receptor kinase-5) and type II (BMP receptor type II) membrane serine/threonine kinase receptors [46, 47], resulting in the phosphorylation and activation of SMAD protein [48]. In the present study, we showed that GDF9 could perform the function of inhibiting BIM_{EL} expression of oocytes via activating PI3K signal pathway. Orisaka et al. [27] inferred that this process might involve SMAD3-mediated down-regulation of phosphatase and tensin homolog (a tumor suppressor that negatively regulates phosphoinositide phosphorylation). However, phosphorylation of FOXO3a was not affected by SMAD inhibitor in the presence of GDF9, which suggested that activation of PI3K by GDF9 appeared to be independent of SMAD activation. Wilkes et al. [49] found that activation of PI3K pathway by TGFβ in AKR-2B fibroblasts was required for p21-activated kinase-2 kinase rather than SMAD activity. Whether this indeed is the case in the cumulus cells awaits further investigation.

Our results demonstrated that GDF9 inhibited BIM_{EL} expression and thus possessed antiapoptotic actions. In a study using bovine COCs, GDF9 had no significant effect on cumulus cell apoptosis whereas two other OSFs (i.e., BMP15 and BMP6) reduced cumulus cell apoptosis [14]. However, in a study using rat preantral follicles, GDF9 was shown to exert antiapoptotic effects in preantral follicles and protected granulosa cells from undergoing apoptosis [27]. Differences between the antiapoptotic actions of GDF9 in these two reports might suggest that there were differences in GDF9 antiapoptotic activity between species or might suggest that GDF9 had antiapoptotic actions during early but not late stages of follicle development [50].

We also showed that PDTC, a nuclear factor kappa B (NFκB) inhibitor, could also dampen the inhibitory action of GDF9 on BIM_{EL} expression. Unlike another chemical inhibitor, such as LY294002, which promoted the target transcriptional factor FOXO3a activation, PDTC prevented NFκB nuclear translocation [51]. Thus, we inferred that NFκB functions as a transcriptional repressor for *BIM* gene, which was verified by the down-regulation of BIM protein by NFκB p65 subunit overexpression (data not shown). This is in line with the central theme of NFκB biology, which portrays NFκB as being oncogenic and antiapoptotic [52]. However, Inta et al. [53] indicated that NFκB could bind to the *BIM* promoter and stimulate gene transcription in primary cortical neurons, suggesting that NFκB fine-tune activation was dependent on the cell type or the nature of the apoptotic stimulus. Lee et al. [54] showed that NFκB could bind the antiapoptotic gene *BCL2L1* promoter and support its transcriptional activity during CD40-mediated B lymphocytes survival. The conflicting results from Campbell et al. [55] indicated that NFκB induced by cytotoxic stimuli such as ultraviolet light and certain chemotherapeutic drugs like daunorubicin and doxorubicin was a repressor of *BCL2L1* transcription in human osteosarcoma cells. It is intriguing that the same transcriptional factor is able to mediate both transcriptional activation and repression of same gene in a promoter-specific manner. In this regard, whether NFκB pathway is regulated by OSFs is as yet unknown and will form the basis of further investigations concerning the detailed mechanism of the regulation of BIM_{EL} expression by NFκB in cumulus cells.

Follicular somatic cells rapidly lose gonadotropin receptor in in vitro culture conditions [56]. In most previously described culture systems, granulosa cells slightly respond only to pharmacological doses of gonadotropin [57–59]. In our present experimental system, we also only detected the slightly decreasing BIM_{EL} expression by a high dose of GDF9 (1000 ng/ml) in cultured monolayers of cumulus cells (data not shown). Perhaps this is the reason why subsequently GDF9 suppressing reporter activity is minor in cumulus monolayer transfected with constructs. Objectively, we indeed showed GDF-9 significantly ($P < 0.05$) reduced −254 and +62 bp region dependent activation, which was verified by increasing phospho-FOXO3a content induced by GDF9 in OOXs (Fig. 5).

In summary, we showed that the cumulus cell apoptosis inhibited by oocyte involved down-regulating BIM_{EL} expression via the PI3K/FOXO3a pathway. This work provides new insight into how the BCL-2 protein family, especially BIM, functions in cumulus cells.

REFERENCES

1. Eppig J. Oocyte control of ovarian follicular development and function in mammals. Reproduction 2001; 122:829–838.
2. Matzuk MM, Burns KH, Viveiros MM, Eppig JJ. Intercellular communication in the mammalian ovary: oocytes carry the conversation. Science 2002; 296:2178–2180.
3. Gilchrist RB, Thompson JG. Oocyte maturation: emerging concepts and technologies to improve developmental potential in vitro. Theriogenology 2007; 67:6–15.
4. Gilchrist RB, Lane M, Thompson JG. Oocyte-secreted factors: regulators of cumulus cell function and oocyte quality. Hum Reprod Update 2008; 14:159–177.
5. Yeo CX, Gilchrist RB, Lane M. Disruption of bidirectional oocyte-cumulus paracrine signaling during in vitro maturation reduces subsequent

mouse oocyte developmental competence. Biol Reprod 2009; 80: 1072–1080.
6. Brower PT, Schultz RM. Intercellular communication between granulosa cells and mouse oocytes: existence and possible nutritional role during oocyte growth. Dev Biol 1982; 90:144–153.
7. Kimura N, Hoshino Y, Totsukawa K, Sato E. Cellular and molecular events during oocyte maturation in mammals: molecules of cumulus-oocyte complex matrix and signalling pathways regulating meiotic progression. Soci Reprod Fertil Suppl 2007; 63:327–342.
8. Eppig JJ, Wigglesworth K, Pendola FL. The mammalian oocyte orchestrates the rate of ovarian follicular development. Proc Natl Acad Sci U S A 2002; 99:2890–2894.
9. Soyal SM, Amleh A, Dean J. FIGalpha, a germ cell-specific transcription factor required for ovarian follicle formation. Development 2000; 127: 4645–4654.
10. Latham KE, Wigglesworth K, McMenamin M, Eppig JJ. Stage-dependent effects of oocytes and growth differentiation factor 9 on mouse granulosa cell development: advance programming and subsequent control of the transition from preantral secondary follicles to early antral tertiary follicles. Biol Reprod 2004; 70:1253–1262.
11. Diaz FJ, O'Brien MJ, Wigglesworth K, Eppig JJ. The preantral granulosa cell to cumulus cell transition in the mouse ovary: development of competence to undergo expansion. Dev Biol 2006; 299:91–104.
12. Sugiura K, Pendola FL, Eppig JJ. Oocyte control of metabolic cooperativity between oocytes and companion granulosa cells: energy metabolism. Dev Biol 2005; 279:20–30.
13. Su Y-Q, Sugiura K, Wigglesworth K, O'Brien MJ, Affourtit JP, Pangas SA, Matzuk MM, Eppig JJ. Oocyte regulation of metabolic cooperativity between mouse cumulus cells and oocytes: BMP15 and GDF9 control cholesterol biosynthesis in cumulus cells. Development 2008; 135: 111–121.
14. Hussein TS, Froiland DA, Amato F, Thompson JG, Gilchrist RB. Oocytes prevent cumulus cell apoptosis by maintaining a morphogenic paracrine gradient of bone morphogenetic proteins. J Cell Sci 2005; 118:5257–5268.
15. Yang MY, Rajamahendran R. Morphological and biochemical identification of apoptosis in small, medium, and large bovine follicles and the effects of follicle-stimulating hormone and insulin-like growth factor-I on spontaneous apoptosis in cultured bovine granulosa cells. Biol Reprod 2000; 62:1209–1217.
16. Durlinger AL, Kramer P, Karels B, Grootegoed JA, Uilenbroek JT, Themmen AP. Apoptotic and proliferative changes during induced atresia of pre-ovulatory follicles in the rat. Hum Reprod 2000; 15:2504–2511.
17. Kugu K, Ratts VS, Piquette GN, Tilly KI, Tao XJ, Martimbeau S, Aberdeen GW, Krajewski S, Reed JC, Pepe GJ, Albrecht ED, Tilly JL. Analysis of apoptosis and expression of bcl-2 gene family members in the human and baboon ovary. Cell Death Differ 1998; 5:67–76.
18. Cory S, Adams JM. The Bcl2 family: regulators of the cellular life-or-death switch. Nat Rev Cancer 2002; 2:647–656.
19. O'Connor L, Strasser A, O'Reilly LA, Hausmann G, Adams JM, Cory S, Huang DC. BIM: a novel member of the Bcl-2 family that promotes apoptosis. EMBO J 1998; 17:384–395.
20. O'Reilly LA, Cullen L, Visvader J, Lindeman GJ, Print C, Bath ML, Huang DC, Strasser A. The proapoptotic BH3-only protein bim is expressed in hematopoietic, epithelial, neuronal, and germ cells. Am J Pathol 2000; 157:449–461.
21. Wang XL, Wu Y, Tan LB, Tian Z, Liu JH, Zhu DS, Zeng SM. Follicle-stimulating hormone regulates pro-apoptotic protein Bcl-2-interacting mediator of cell death-extra long (BimEL)-induced porcine granulosa cell apoptosis. J Biol Chem 2012; 287:10166–10177.
22. Wu Y, Wang XL, Liu JH, Bao ZJ, Tang DW, Wu Y, Zeng SM. BIM EL-mediated apoptosis in cumulus cells contributes to degenerative changes in aged porcine oocytes via a paracrine action. Theriogenology 2011; 76: 1487–1495.
23. Vanderhyden BC. Molecular basis of ovarian development and function. Front Biosci 2002; 7:2006–2022.
24. Diaz FJ, Wigglesworth K, Eppig JJ. Oocytes determine cumulus cell lineage in mouse ovarian follicles. J Cell Sci 2007; 120:1330–1340.
25. Sasseville M, Ritter LJ, Nguyen TM, Liu F, Mottershead DG, Russell DL, Gilchrist RB. Growth differentiation factor 9 signaling requires ERK1/2 activity in mouse granulosa and cumulus cells. J Cell Sci 2010; 123: 3166–3176.
26. Zhang YE. Non-Smad pathways in TGF-beta signaling. Cell Res 2009; 19:128–139.
27. Orisaka M, Orisaka S, Jiang JY, Craig J, Wang Y, Kotsuji F, Tsang BK. Growth differentiation factor 9 is antiapoptotic during follicular development from preantral to early antral stage. Mol Endocrinol 2006; 20:2456–2468.
28. Akiyama T, Dass CR, Choong P. Bim-targeted cancer therapy: a link between drug action and underlying molecular changes. Mol Cancer Ther 2009; 8:3173–3180.
29. Boni R, Cuomo A, Tosti E. Developmental potential in bovine oocytes is related to cumulus-oocyte complex grade, calcium current activity, and calcium stores. Biol Reprod 2002; 66:836–842.
30. Yamashita Y, Hishinuma M, Shimada M. Activation of PKA, p38 MAPK and ERK1/2 by gonadotropins in cumulus cells is critical for induction of EGF-like factor and TACE/ADAM17 gene expression during in vitro maturation of porcine COCs. J Ovarian Res 2009; 2:20.
31. Su YQ, Sugiura K, Li Q, Wigglesworth K, Matzuk MM, Eppig JJ. Mouse oocytes enable LH-induced maturation of the cumulus-oocyte complex via promoting EGF receptor-dependent signaling. Mol Endocrinol 2010; 24: 1230–1239.
32. Cuervo AM, Hu W, Lim B, Dice JF. IkB is a substrate for a selective pathway of lysosomal proteolysis. Mol Biol Cell 1998; 9:1995–2010.
33. Zhang X, Miao Y, Zhao JG, Spate L, Bennett MW, Murphy CN, Schatten H, Prather RS. Porcine oocytes denuded before maturation can develop to the blastocyst stage if provided a cumulous cell-derived coculture system. J Anim Sci 2010; 88:2604–2610.
34. Prochazka R, Blaha M, Nemcova L. Signaling pathways regulating FSH and amphiregulin induced meiotic resumption and cumulus cell expansion in the pig. Reproduction 2012; 144:535–546.
35. Purcell SH, Chi MM, Moley KH. Insulin-stimulated glucose uptake occurs in specialized cells within the cumulus oocyte complex. Endocrinology 2012; 153:2444–2454.
36. Calnan DR, Brunet A. The FoxO code. Oncogene 2008; 27:2276–2288.
37. Manabe N, Imai Y, Ohno H, Takahagi Y, Sugimoto M, Miyamoto H. Apoptosis occurs in granulosa cells but not cumulus cells in the atretic antral follicles in pig ovaries. Experientia 1996; 52:647–651.
38. Dong J, Albertini DF, Nishimori K, Kumar TR, Lu N, Matzuk MM. Growth differentiation factor-9 is required during early ovarian folliculogenesis. Nature 1996; 383:531–535.
39. Galloway SM, McNatty KP, Cambridge LM, Laitinen MP, Juengel JL, Jokiranta TS, McLaren RJ, Luiro K, Dodds KG, Montgomery GW, Beattie AE, Davis GH, et al. Mutations in an oocyte-derived growth factor gene (BMP15) cause increased ovulation rate and infertility in a dosage-sensitive manner. Nat Genet 2000; 25:279–283.
40. McPherron AC, Lee SJ. GDF-3 and GDF-9: two new members of the transforming growth factor-beta superfamily containing a novel pattern of cysteines. J Biol Chem 1993; 268:3444–3449.
41. Shimizu T, Miyahayashi Y, Yokoo M, Hoshino Y, Sasada H, Sato E. Molecular cloning of porcine growth differentiation factor 9 (GDF-9) cDNA and its role in early folliculogenesis: direct ovarian injection of GDF-9 gene fragments promotes early folliculogenesis. Reproduction 2004; 128:537–543.
42. Hickey TE, Marrocco DL, Amato F, Ritter LJ, Norman RJ, Gilchrist RB, Armstrong DT. Androgens augment the mitogenic effects of oocyte-secreted factors and growth differentiation factor 9 on porcine granulosa cells. Biol Reprod 2005; 73:825–832.
43. Hershko T, Ginsberg D. Up-regulation of Bcl-2 homology 3 (BH3)-only proteins by E2F1 mediates apoptosis. J Biol Chem 2004; 279:8627–8634.
44. Hughes R, Kristiansen M, Lassot I, Desagher S, Mantovani R, Ham J. NF-Y is essential for expression of the proapoptotic bim gene in sympathetic neurons. Cell Death Differ 2011; 18:937–947.
45. Gilley J, Coffer PJ, Ham J. FOXO transcription factors directly activate bim gene expression and promote apoptosis in sympathetic neurons. J Cell Biol 2003; 162:613–622.
46. Mazerbourg S, Klein C, Roh J, Kaivo-Oja N, Mottershead DG, Korchynskyi O, Ritvos O, Hsueh AJ. Growth differentiation factor-9 signaling is mediated by the type I receptor, activin receptor-like kinase 5. Mol Endocrinol 2004; 18:653–665.
47. Vitt UA, Mazerbourg S, Klein C, Hsueh AJ. Bone morphogenetic protein receptor type II is a receptor for growth differentiation factor-9. Biol Reprod 2002; 67:473–480.
48. Roh JS, Bondestam J, Mazerbourg S, Kaivo-Oja N, Groome N, Ritvos O, Hsueh AJ. Growth differentiation factor-9 stimulates inhibin production and activates Smad2 in cultured rat granulosa cells. Endocrinology 2003; 144:172–178.
49. Wilkes MC, Mitchell H, Penheiter SG, Doré JJ, Suzuki K, Edens M, Sharma DK, Pagano RE, Leof EB. Transforming growth factor-beta activation of phosphatidylinositol 3-kinase is independent of Smad2 and Smad3 and regulates fibroblast responses via p21-activated kinase-2. Cancer Res 2005; 65:10431–10440.
50. Otsuka F, McTavish K, Shimasaki S. Integral role of GDF-9 and BMP-15 in ovarian function. Mol Reprod Dev 2011; 78:9–21.
51. Nurmi A, Vartiainen N, Pihlaja R, Goldsteins G, Yrjanheikki J, Koistinaho

J. Pyrrolidine dithiocarbamate inhibits translocation of nuclear factor kappa-B in neurons and protects against brain ischaemia with a wide therapeutic time window. J Neurochem 2004; 91:755–765.
52. Kucharczak J, Simmons MJ, Fan Y, Gelinas C. To be, or not to be: NF-kappaB is the answer—role of Rel/NF-kappaB in the regulation of apoptosis. Oncogene 2003; 22:8961–8982.
53. Inta I, Paxian S, Maegele I, Zhang W, Pizzi M, Spano P, Sarnico I, Muhammad S, Herrmann O, Inta D, Baumann B, Liou HC, et al. Bim and Noxa are candidates to mediate the deleterious effect of the NF-kappa B subunit RelA in cerebral ischemia. J Neurosci 2006; 26:12896–12903.
54. Lee HH, Dadgostar H, Cheng Q, Shu J, Cheng G. NF-kappaB-mediated up-regulation of Bcl-x and Bfl-1/A1 is required for CD40 survival signaling in B lymphocytes. Proc Natl Acad Sci U S A 1999; 96: 9136–9141.
55. Campbell KJ, Rocha S, Perkins ND. Active repression of antiapoptotic gene expression by RelA(p65) NF-kappa B. Mol Cell 2004; 13:853–865.
56. Lie BL, Leung E, Leung PC, Auersperug N. Long-term growth and steroidogenic potential of human granulosa-lutein cells immortalized with SV40 large T antigen. Mol Cell Endocrinol 1996; 120:169–176.
57. Gong JG, McBride D, Bramley TA, Webb R. Effects of recombinant bovine somatotrophin, insulin-like growth factor-I and insulin on bovine granulosa cell steroidogenesis in vitro. J Endocrinol 1994; 143:157–164.
58. Vernon RK, Spicer LJ. Effects of basic fibroblast growth factor and heparin on follicle-stimulating hormone-induced steroidogenesis by bovine granulosa cells. J Anim Sci 1994; 72:2696–2702.
59. Alpizar E, Spicer LJ. Effects of interleukin-6 on proliferation and follicle-stimulating hormone-induced estradiol production by bovine granulosa cells in-vitro: dependence on size of follicle. Biol Reprod 1993; 49:38–43.